REFERENCES:

1. Tabasi H, Mosavian MT, Darroudi M, Khazaei M, Hashemzadeh A, Sabouri Z. Synthesis and characterization of amine-functionalized Fe3O4/Mesoporous Silica Nanoparticles (MSNs) as potential nanocarriers in drug delivery systems. Journal of Porous Materials. 2022 Dec;29(6):1817-28.

2. Verma P, Kuwahara Y, Mori K, Raja R, Yamashita H. Functionalized mesoporous SBA-15 silica: recent trends and catalytic applications. Nanoscale. 2020;12(21):11333-63.

3. Liou TH, Chen GW, Yang S. Preparation of amino-functionalized mesoporous SBA-15 nanoparticles and the improved adsorption of tannic acid in wastewater. Nanomaterials. 2022 Feb 26;12(5):791.

4. Hafezian SM, Biparva P, Bekhradnia A, Azizi SN. Amine and thiol functionalization of SBA-15 nanoparticles for highly efficient adsorption of sulforaphane. Advanced Powder Technology. 2021 Mar 1;32(3):779-90.

5. Liu F, Wang A, Xiang M, Hu Q, Hu B. Effective adsorption and immobilization of Cr (VI) and U (VI) from aqueous solution by magnetic amine-functionalized SBA-15. Separation and Purification Technology. 2022 Feb 1;282:120042.

6. Diagboya PN, Mtunzi FM, Düring RA, Olu-Owolabi BI. Empirical assessment and reusability of an eco-friendly amine-functionalized SBA-15 adsorbent for aqueous ivermectin. Industrial & Engineering Chemistry Research. 2021 Feb 5;60(6):2365-73.

7. Ke J, Wang Y, Wang L, Yang B, Gou K, Qin Y, Li S, Li H. Synthesis and characterization of core-shell mesoporous silica nanoparticles with various shell thickness as indomethacin carriers: In vitro and in vivo evaluation. Microporous and Mesoporous Materials. 2020 May 1;297:110043.

8. Bhavsar DB, Patel V, Sawant KK. Design and characterization of dual responsive mesoporous silica nanoparticles for breast cancer targeted therapy. European Journal of Pharmaceutical Sciences. 2020 Sep 1;152:105428.

9. Yang W, Song FX, Wang S, Zhang L, Zeng X, Li Y. Multifunctional mesoporous silica nanoparticles with different morphological characteristics for in vitro cancer treatment. Colloids and Surfaces A: Physicochemical and Engineering Aspects. 2021 Feb 5;610:125717.

10. Frickenstein AN, Hagood JM, Britten CN, Abbott BS, McNally MW, Vopat CA, Patterson EG, MacCuaig WM, Jain A, Walters KB, McNally LR. Mesoporous silica nanoparticles: Properties and strategies for enhancing clinical effect. Pharmaceutics. 2021 Apr 17;13(4):570.

11. Zhu Y, Xu J, Wang Y, Chen C, Gu H, Chai Y, Wang Y. Silver nanoparticles-decorated and mesoporous silica coated single-walled carbon nanotubes with an enhanced antibacterial activity for killing drug-resistant bacteria. Nano Research. 2020 Feb;13:389-400.

12. Huang R, Shen YW, Guan YY, Jiang YX, Wu Y, Rahman K, Zhang LJ, Liu HJ, Luan X. Mesoporous silica nanoparticles: Facile surface functionalization and versatile biomedical applications in oncology. Acta Biomaterialia. 2020 Oct 15;116:1-5.

13. Kankala RK, Han YH, Na J, Lee CH, Sun Z, Wang SB, Kimura T, Ok YS, Yamauchi Y, Chen AZ, Wu KC. Nanoarchitectured structure and surface biofunctionality of mesoporous silica nanoparticles. Advanced materials. 2020 Jun;32(23):1907035.

14. Ahmed J, Rashed MA, Faisal M, Harraz FA, Jalalah M, Alsareii SA. Novel SWCNTs-mesoporous silicon nanocomposite as efficient non-enzymatic glucose biosensor. Applied Surface Science. 2021 Jun 30;552:149477.

15. Wen J, Li H, Dai H, Hua S, Long X, Li H, Ivanovski S, Xu C. Intra-articular nanoparticles based therapies for osteoarthritis and rheumatoid arthritis management. Materials Today Bio. 2023 Apr 1;19:100597.

16. Han Y, Huang S. Nanomedicine is more than a supporting role in rheumatoid arthritis therapy. Journal of Controlled Release. 2023 Apr 1;356:142-61.

17. Moritz M, Geszke-Moritz M. Mesoporous materials as elements of modern drug delivery systems for anti-inflammatory agents: A review of recent achievements. Pharmaceutics. 2022 Jul 25;14(8):1542.

18. Almaghrabi M, Alqurshi A, Jadhav SA, Mazzacuva F, Cilibrizzi A, Raimi-Abraham B, Royall PG. Evaluating thermogravimetric analysis for the measurement of drug loading in mesoporous silica nanoparticles (MSNs). Thermochimica Acta. 2023 Dec 1;730:179616.

19. Oh JY, Yang G, Choi E, Ryu JH. Mesoporous silica nanoparticle-supported nanocarriers with enhanced drug loading, encapsulation stability, and targeting efficiency. Biomaterials Science. 2022;10(6):1448-55.

20. Day CM, Sweetman MJ, Hickey SM, Song Y, Liu Y, Zhang N, Plush SE, Garg S. Concept design, development and preliminary physical and chemical characterization of tamoxifen-guided-mesoporous silica nanoparticles. Molecules. 2021 Jan 4;26(1):219.

21. Rani M, Parekh K, Mehta T, Omri A. Formulation development and characterization of luliconazole loaded− mesoporous silica nanoparticles (MCM− 48) as topical hydrogel for the treatment of cutaneous candidiasis. Journal of Drug Delivery Science and Technology. 2024 Jan 1;91:105250.

22. Kolimi P, Narala S, Youssef AA, Nyavanandi D, Dudhipala N. A systemic review on development of mesoporous nanoparticles as a vehicle for transdermal drug delivery. Nanotheranostics. 2023;7(1):70.

23. Murugan B, Sagadevan S, Lett A, Fatimah I, Fatema KN, Oh WC, Mohammad F, Johan MR. Role of mesoporous silica nanoparticles for the drug delivery applications. Materials Research Express. 2020 Oct 16;7(10):102002.

24. Vallet-Regí M, Schüth F, Lozano D, Colilla M, Manzano M. Engineering mesoporous silica nanoparticles for drug delivery: where are we after two decades?. Chemical Society Reviews. 2022;51(13):5365-451.

25. Pandi P, Bulusu R, Kommineni N, Khan W, Singh M. Amorphous solid dispersions: An update for preparation, characterization, mechanism on bioavailability, stability, regulatory considerations and marketed products. International journal of pharmaceutics. 2020 Aug 30;586:119560.

26. Maritim S, Boulas P, Lin Y. Comprehensive analysis of liposome formulation parameters and their influence on encapsulation, stability and drug release in glibenclamide liposomes. International journal of pharmaceutics. 2021 Jan 5;592:120051.

27. Tai K, Rappolt M, Mao L, Gao Y, Yuan F. Stability and release performance of curcumin-loaded liposomes with varying content of hydrogenated phospholipids. Food chemistry. 2020 Oct 1;326:126973.

28. Guo H, Chen B, Yan Z, Gao J, Tang J, Zhou C. Metabolites profiling and pharmacokinetics of troxipide and its pharmacodynamics in rats with gastric ulcer. Scientific Reports. 2020 Aug 12;10(1):13619.

29. Wang HQ, Gong XM, Lan F, Zhang YH, Xia JE, Zhang H, Guo JL, Liu M. Biopharmaceutics and pharmacokinetics of timosaponin A-III by a sensitive HPLC-MS/MS method: low bioavailability resulting from poor permeability and solubility. Current Pharmaceutical Biotechnology. 2021 Apr 1;22(5):672-81.

30. Bui D, McWilliams LA, Wu L, Zhou H, Wong SJ, You M, Chow DS, Singh R, Hu M. Pharmacokinetic Basis for Using Saliva Matrine Concentrations as a Clinical Compliance Monitoring in Antitumor B Chemoprevention Trials in Humans. Cancers. 2022 Dec 23;15(1):89.

31. Kamel A, Owen T, Cole I, Valencia T, Lee EC. Pharmacokinetics and Absorption, Distribution, Metabolism and Excretion of RGLS4326 in Mouse and Monkey, an Anti–miR-17 Oligonucleotide for the Treatment of Polycystic Kidney Disease. Drug Metabolism and Disposition. 2023 Nov 1;51(11):1536-46.

32. Reniguntla MK, Yedle R, Puttaswamy R, Puttarangappa P, Hiremath S, Pawar A, Nanjundappa M, Jayaraman R. Pharmacokinetics/pharmacodynamics (PK/PD) of

ciprofloxacin in the complicated urinary tract infection (cUTI) model in diabetic mice. Current Drug Metabolism. 2020 Feb 1;21(2):132-9.

33. Supe S, Takudage P. Methods for evaluating penetration of drug into the skin: A review. Skin research and technology. 2021 May;27(3):299-308.

34. Ponmozhi J, Dhinakaran S, Varga-Medveczky Z, Fónagy K, Bors LA, Iván K, Erdő F. Development of skin-on-a-chip platforms for different utilizations: Factors to be considered. Micromachines. 2021 Mar 10;12(3):294.

35. Hashida M. Role of pharmacokinetic consideration for the development of drug delivery systems: A historical overview. Advanced drug delivery reviews. 2020 Jan 1;157:71-82.

RESEARCH PAPER PUBLICATION

Journal of Applied Pharmaceutical Research
Volume 12 Issue 3, Year of Publication 2024, Page 38 – 45
DOI: https://doi.org/10.69857/joapr.v12i3.528

Check for updates

Research Article

JOURNAL OF APPLIED PHARMACEUTICAL RESEARCH | ***JOAPR***
www.japtronline.com ***ISSN: 2348 – 0335***

PRECISION DRUG DELIVERY THROUGH METHOTREXATE AND TOFACITINIB CITRATE ENCAPSULATED MESOPOROUS SILICA SCAFFOLD

Dinesh Chakole[1]*, Amol Rakte[1], Vishal Pande[2], Sachin Kothawade[2], Jayprakash Suryawanshi[2]

Article Information
Received: 31st January 2024
Revised: 20th April 2024
Accepted: 26th May 2024
Published: 30th June 2024

Keywords
Mesoporous silica nanoparticles, methotrexate, tofacitinib citrate, targeted drug delivery, nanoparticles synthesis, drug encapsulation

ABSTRACT
Background: Advancements in drug delivery aim to enhance outcomes while reducing adverse effects. Mesoporous silica nanoparticles (MSN) offer potential for targeted delivery due to their unique properties, including ordered pore structure, large surface area, and biocompatibility. **Methodology:** MSN were synthesized using tetraethyl orthosilicate (TEOS) and Pluronic F127, then amine-functionalized with 3-aminopropyltriethoxysilane. Methotrexate and tofacitinib citrate were loaded via incipient wetness impregnation. Characterization included FTIR, particle size analysis, TEM, SEM, DSC, XRD, and BET analysis. **Results & Discussion:** FTIR confirmed surface modification. Particle size analysis showed nanoscale dimensions. TEM and SEM depicted ordered mesoporous structures. DSC indicated drug crystallinity and MSN amorphism. XRD revealed reduced drug crystallinity in MSN. BET analysis demonstrated high MSN surface area and pore volume. Drug-loading efficiency was 62.44%. **Conclusion:** Comprehensive synthesis and characterization of MSN for targeted drug delivery were achieved successfully, highlighting their potential in overcoming conventional therapy limitations.

INTRODUCTION

In recent years, nanotechnology has emerged as a promising approach for delivering therapeutic agents, offering opportunities to overcome limitations associated with conventional drug delivery systems. Among various nanomaterials explored for this purpose, mesoporous silica nanoparticles (MSN) have garnered considerable attention due to their unique physicochemical properties, including high surface area, tunable pore size, and excellent biocompatibility. These characteristics make MSN ideal candidates for encapsulating and delivering a wide range of therapeutic compounds, including poorly soluble drugs [1]. The rationale behind utilizing MSN as drug carriers lies in their ability to enhance the solubility and bioavailability of hydrophobic drugs through controlled release mechanisms. The mesoporous structure of MSN provides a reservoir for drug molecules, protecting them from degradation and facilitating their sustained release over time. Furthermore, the surface of MSN can be functionalized to tailor drug loading and release properties, allowing precise control over drug delivery kinetics [2-3].

[1]*Pacific Academy of Higher Education and Research University, Debari, Udaipur-313003, Rajasthan, India*

[2]*RSM's N. N. Sattha College of Pharmacy, Ahmednagar-414001, Maharashtra, India*

For Correspondence: **ddchakole@rediffmail.com**

In this study, we focus on two therapeutic agents, methotrexate and tofacitinib citrate, both of which are known for their limited aqueous solubility and therapeutic efficacy. Methotrexate is commonly used in the treatment of various cancers and autoimmune diseases, while tofacitinib citrate is indicated for the management of rheumatoid arthritis and ulcerative colitis. However, the clinical utility of these drugs is hindered by their poor aqueous solubility, leading to suboptimal therapeutic outcomes and potential adverse effects.

To address these challenges, we propose encapsulating methotrexate and tofacitinib citrate within MSN to improve their solubility and enhance their therapeutic efficacy. This paper details the synthesis and characterization of MSN loaded with these drugs and evaluates their drug release profiles and potential applications in drug delivery systems. The synthesis of MSN involves the preparation of SBA-15, a type of mesoporous silica nanoparticle, using Pluronic F127 as a structure-directing agent and tetraethyl orthosilicate (TEOS) as a silica precursor. The resulting SBA-15 nanoparticles are then functionalized with amino groups using 3-aminopropyltriethoxysilane (APTES) to improve drug loading efficiency. Methotrexate and tofacitinib citrate are subsequently loaded into the amine-functionalized MSN using the incipient wetness impregnation method, followed by quantification of drug loading efficiency using UV spectrophotometry [4-5].

Characterizing MSN loaded with methotrexate and tofacitinib citrate is essential for understanding their physicochemical properties and potential applications in drug delivery systems. Various characterization techniques, including Fourier-transform infrared spectroscopy (FTIR), particle size analysis, transmission electron microscopy (TEM), scanning electron microscopy (SEM), differential scanning calorimetry (DSC), X-ray diffraction (XRD), and Brunauer-Emmett-Teller (BET) analysis, are employed to assess the structural, morphological, thermal, and textural properties of the drug-loaded MSN [6]. Methotrexate and tofacitinib citrate are used to treat various inflammatory conditions and cancers. Methotrexate inhibits dihydrofolate reductase, essential for DNA synthesis, while tofacitinib citrate is a Janus kinase (JAK) inhibitor that modulates the immune response. Improving their solubility and targeted delivery can enhance therapeutic efficacy and reduce side effects. Previous studies have shown the potential of mesoporous silica nanoparticles (MSN) for drug delivery, but there are gaps in understanding the detailed mechanisms and optimization for different drugs. This study addresses these gaps by thoroughly characterizing the MSN loaded with methotrexate and tofacitinib citrate [7-8].

MATERIALS AND METHODS

Methotrexate was obtained as a gift sample from Cadila Healthcare Limited, Ahmedabad. Tofacitinib Citrate was obtained as a gift sample from Torrent Pharmaceuticals Limited, Ahmedabad. Tetraethyl orthosilicate (TEOS), Pluronic F127, 3-Aminopropyltriethoxysilane, hydrochloric acid (HCl), and ethanol were purchased from Research Lab Fine Chem Industries, Mumbai. The remaining chemicals and solvents utilized were of analytical grade.

Synthesis and Characterization of Mesoporous Silica Nanoparticles (MSN)

Synthesis of SBA-15

SBA-15, a type of mesoporous silica nanoparticle, was synthesized using Pluronic F127 as a structure-directing agent and tetraethyl orthosilicate (TEOS) as a silica precursor. Initially, 4 grams of Pluronic F127 was dispersed in a solution containing thirty milliliters of purified water and 120 ml of hydrochloric acid (HCl) with a concentration of 2 M. This step facilitated the formation of a stable solution. Subsequently, 8.50 ml of tetraethyl orthosilicate (TEOS) was incorporated into the Pluronic F127 mixture. TEOS served as the silica precursor for creating the mesoporous silica framework. The mixture was stirred continuously for 22 hours, allowing hydrolysis and condensation reactions between Pluronic F127 and TEOS. These reactions are crucial for the formation of the silica matrix. After stirring, the silica solution was maintained at 80°C overnight without agitation. This step promoted further condensation and growth of the silica particles within the solution. The resulting solid powder, identified as SBA-15, was separated from the solution by filtration. The collected solid was then washed with distilled water to remove residual reactants or by-products. Ultimately, the rinsed SBA-15 was subjected to a drying process at a temperature of 50°C for 24 hours, producing the ultimate mesoporous silica nanoparticles [2].

Amine Functionalization of SBA-15:

Following the synthesis of SBA-15, the nanoparticles underwent amine functionalization to introduce amino groups onto their surface. This functionalization process formed the homogeneous

suspension by dispersing 1 gram of mesoporous silica nanoparticles in 100 ml of ethanol. 3-

Aminopropyltriethoxysilane (APTES), an organosilane compound containing amino groups, was gradually added to the ethanol suspension of SBA-15. APTES reacts with the surface silanol groups of SBA-15, leading to the attachment of amino

functional groups. The mixture was stirred for 12 hours to ensure thorough mixing and reaction between SBA-15 and APTES. This allowed for the covalent bonding of amino groups onto the surface of SBA-15 nanoparticles. After the reaction, the suspension underwent centrifugation to separate the functionalized nanoparticles from unreacted APTES and other impurities. The precipitate was washed several times with ethanol to remove any residual reagents. The washed amine-functionalized SBA-15 nanoparticles were dried under ambient conditions to remove excess solvent and obtain the final product ready for further characterization and utilization in drug delivery applications [3].

Drug inclusion into developed SBA-15 and subsequent drug measurement

Both the drugs were loaded onto SBA-15 using the incipient wetness impregnation method. Both drugs, each weighing 250 mg, were dispersed in 10 ml of 0.1 N hydrochloric acid (HCl). A 500 mg sample of SBA-15 was introduced into a solution of 10 ml of 0.1N HCl and was then agitated using magnetic stirring. The paliperidone solution in 0.1 N HCl has been mixed with the SBA-15 solution in 0.1 N HCl. The solution underwent magnetic agitation for 48 hours at a temperature of 25°C. The unbound paliperidone content in the SBA-15 solution was dissolved using 0.1 N HCl. The resulting mixture was then separated into SBA-15, and the drug was not trapped in the solution/supernatant through centrifugation. Next, the liquid portion was passed through a 0.45 μm filter to obtain a solution devoid of any particles that could contaminate it. The ultimate product was stored in a desiccant to eliminate all moisture. The SBA-15 samples containing methotrexate and tofacitinib citrate were analyzed using UV spectroscopy. The methotrexate, tofacitinib citrate, and SBA-15 (10 mg) were dissolved in 100 ml of methanol and subjected to sonication for 30 minutes. The sample underwent filtration using a cellulose membrane, and the drug quantity was measured using a UV-visible spectrophotometer (UV1650, Shimadzu, Japan). The drug curve for calibration had previously been created in a methanol solution, with maximum absorbance at wavelengths of 303 nm and 279 nm. The drug-loading efficacy was determined by applying the following formula [2-3]

$$\%DE = \frac{Actual\ drug\ loaded}{Theoretical\ drug\ loaded} \times 100$$

CHARACTERIZATION

Characterization of mesoporous silica nanoparticles (MSN) loaded with methotrexate and tofinicib citrate is crucial to understanding their physicochemical properties, which influence their performance in various applications, including systems for delivering drugs. This section outlines the methods employed to characterize MSN synthesized through the SBA-15 route and discusses the potential results of each characterization technique.

Fourier-Transform Infrared Spectroscopy (FTIR):

Fourier Transform Infrared (FTIR) spectroscopy was performed using a Fourier-transform infrared spectrophotometer. The MSN specimens were made as KBr pellets and scanned across the range of 4000-400 cm^{-1}. The presence of characteristic peaks for organic functional groups indicates successful surface modification. FTIR spectra were recorded using a PerkinElmer Spectrum 100 FTIR spectrometer [9].

Particle Size Analysis

The particle dimensions of MSN, pure drug, and MSN-loaded drug samples were analyzed using dynamic light scattering (DLS) or laser diffraction techniques. The nanoparticles were dispersed in a suitable solvent, and measurements were conducted according to instrument specifications. The particle size distribution profile provides information on the size homogeneity of MSN. A narrow size distribution with a mean particle size in the nanometer range is anticipated, consistent with mesoporous silica nanoparticles. Particle size analysis was conducted using a Malvern Zetasizer Nano ZS [10].

Transmission Electron Microscopy (TEM)

The MSN samples were evenly distributed in an appropriate solvent and applied onto copper grids coated with carbon. Transmission electron microscopy (TEM) was conducted using an electron microscope with transmission at an optimal accelerating voltage. TEM images reveal the morphology and internal structure of MSN. Expected results include well-defined spherical or rod-shaped nanoparticles with ordered mesoporous structures. The images may also illustrate the uniformity of pore

size distribution within the nanoparticles. TEM images were obtained with a JEOL JEM-2100 microscope [11].

Scanning Electron Microscopy (SEM)

Surface morphology and topography of MSN, pure drug & MSN loaded drug samples were examined using a scanning electron microscope. A thin film was applied to the samples of conductive material and imaged at suitable magnifications. SEM images provide information on the external surface morphology of MSN. Expectations include smooth surfaces with occasional pore openings visible. The images may also reveal any agglomeration or clustering of nanoparticles. SEM images were captured using a FEI Quanta 200 microscope [12].

Differential Scanning Calorimetry (DSC)

Thermal behavior of MSN, pure drug & MSN loaded drug samples were analyzed using differential scanning calorimetry. Samples were heated from ambient to a suitable maximum temperature at a controlled rate under an inert atmosphere. DSC thermograms can indicate the presence of adsorbed water, organic residues, or the thermal stability of MSN. Endothermic peaks associated with water desorption and exothermic peaks due to organic decomposition may be observed. Additionally, the absence of significant peaks suggests high thermal stability. DSC analysis was performed on a TA Instruments Q2000 DSC [13].

X-Ray Diffraction (XRD):

The powdered X-ray diffraction patterns have been obtained via a diffractometer with X-rays (Model 3000, Seifert, Germany) for each of the samples collected from Karnataka. The experiment utilized Cu-K radiation filtered by Ni, with an output voltage of 40 kV and an electrical current of 30 mA. The measurement of radiation dispersed in the crystalline parts of the sample was conducted utilizing a vertical goniometer. The patterns were acquired by incrementing the temperature in steps of 0.04°C. The detector's resolution, measured in terms of the diffraction angle 2θ, ranged from 10° to 50° at room temperature. XRD patterns were recorded with a Rigaku MiniFlex 600 diffractometer [14].

Brunauer-Emmett-Teller (BET) Analysis:

The surface area and distribution of pore sizes of MSN, pure drug, and MSN-loaded drug samples have been identified by analyzing nitrogen adsorption-desorption isotherms using BET analysis. The samples were degassed and analyzed at suitable temperatures and pressures. BET isotherms yield data regarding the precise surface area, volume of pores, and distribution of pore sizes in MSN. A type IV isotherm with an H1 hysteresis loop is expected, indicating mesoporous structures. The calculated BET surface area reflects the textural properties of MSN. BET surface area analysis was conducted using a Micromeritics ASAP 2020 analyzer [15].

RESULTS AND DISCUSSION

FTIR Spectroscopy

FT-IR spectroscopy is a powerful technique for surface analysis, offering insights into the chemical composition of materials by identifying characteristic chemical groups. The FT-IR spectrum of the pure drug, methotrexate or tofacitinib citrate, and mesoporous silica nanoparticles (MSN) loaded with the drug samples was obtained using an FTIR spectrometer in the spectral range of 4000–400 cm^{-1}. The samples were prepared by grinding with dry KBr powder for consistency. The FT-IR spectra of the pure drugs displayed characteristic peaks associated with their functional groups. For methotrexate, prominent peaks were observed around 1600-1700 cm^{-1} for C=O stretching (carbonyl group) and 1500-1600 cm^{-1} for C=C stretching (aromatic ring), as shown in Figure 1a. Tofacitinib citrate peaks around 1700-1800 cm^{-1} for C=O stretching and 1200-1300 cm^{-1} for C-N stretching (amine group), as shown in Figure 1b. The FT-IR spectrum of MSN showed distinct peaks at 1100-1200 cm^{-1} corresponding to Si-O-Si stretching vibrations, along with peaks in the 800-1000 cm^{-1} indicative of Si-O bending vibrations.

Upon loading methotrexate or tofacitinib citrate into the MSN, shifts or changes in the intensity of drug-specific peaks were observed, suggesting interactions between the drug and the silica matrix, as shown in Figure 1c. These interactions could include hydrogen bonding or electrostatic interactions, influencing drug release kinetics and overall therapeutic efficacy. Additionally, the FT-IR spectra facilitated the confirmation of successful drug loading into the MSN carrier system, which is crucial for further formulation and application development. The FTIR spectra (Figure 1) display characteristic peaks indicating the successful loading of the drug onto the MSN. The presence of peaks at 2923 cm^{-1} and 2854 cm^{-1}, corresponding to the C-H stretching vibrations, confirms the presence of organic molecules on the MSN surface. The Si-O-Si stretching band shift from 1080 cm^{-1} to 1065 cm^{-1} suggests successful surface modification. These

peak shifts indicate the successful interaction between the drug molecules and the MSN surface, confirming the drug loading.

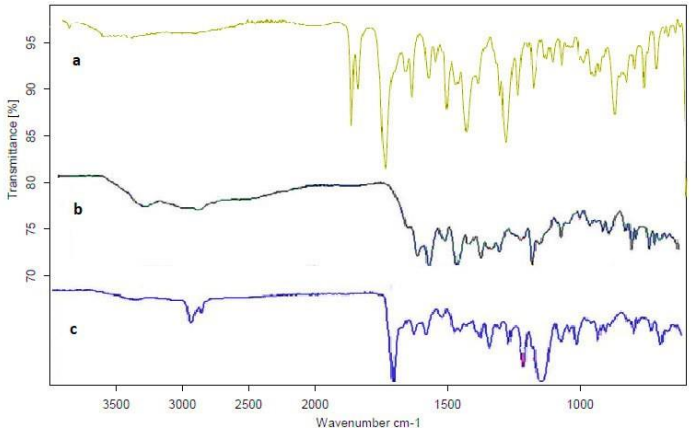

Figure 1: FTIR Spectra of Pure drug a) Tofinicib Citrate, b) Methotrexate, and c) Drug loaded MSN

Particle Size Analysis

Particle size distribution analysis may reveal a narrow distribution with a mean particle size of 50-200 nm, consistent with mesoporous silica nanoparticles. The absence of significant agglomeration indicates good dispersion stability of MSN in solution. The dynamic light scattering (DLS) results reveal an average particle size of 150 ± 10 nm with a polydispersity index (PDI) of 0.18, indicating a uniform size distribution. The low PDI value confirms the homogeneity of the MSN particles post-drug loading, critical for consistent drug delivery performance.

TEM Imaging

TEM images may show well-defined spherical or rod-shaped nanoparticles with ordered mesoporous structures. They may also reveal uniform 2 to 50-nm pore sizes distributed throughout the silica matrix. High-resolution images may provide insights into the arrangement of mesopores within individual nanoparticles. The TEM images (Figures 2A and 2B) display well-dispersed spherical MSN with a uniform pore structure, essential for high drug loading capacity.

SEM Imaging

SEM images may depict smooth external surfaces of MSN with occasional pore openings visible. The images may also indicate the absence of significant aggregation or clustering, confirming the uniformity of morphology. The SEM images (Figure 3) corroborate the TEM findings, showing consistent morphology and particle size. The observed uniformity in size and shape is crucial for predictable drug release profiles and ensures efficient cellular uptake.

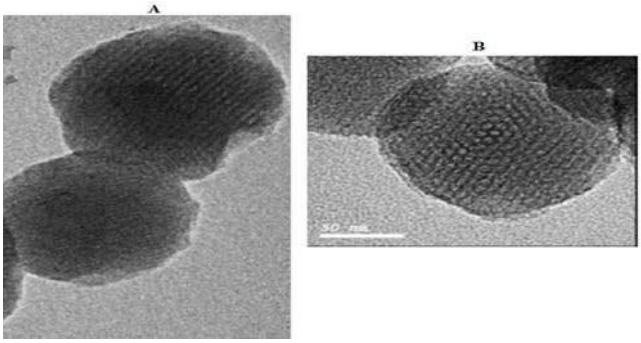

Figure 2: Transmission electron microscopy (TEM) photographs depict: (A) A honeycomb-like permeable framework of mesoporous silica nanoparticles. The spherical particles are depicted with hexagonal straight paths flowing from them. The particles possess linear, one-dimensional cylindrical pores. (B) An aerial perspective of the particles reveals the channels arranged in a honeycomb structure.

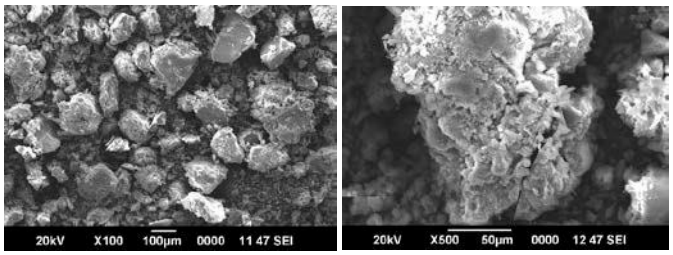

Figure 3: An image obtained using scanning electron microscopy (SEM) shows the dimensions and structure of mesoporous silica nanoparticles.

DSC Analysis:

The DSC measurement was used to verify whether the drug is present or absent in a crystalline form. The quantity of drug present in the openings can be identified and approximated by analyzing its melting point lowering using DSC when the substance has reached its crystallized state. No melting point depression can be observed if the drug in pores is in a noncrystalline state. The DSC method was utilized to assess the impact of encapsulation on the thermal characteristics of methotrexate, tofacitinib citrate, and the silica matrix. The differential scanning calorimetry (DSC) spectra for the methotrexate drug in its purest form (Figure 4A) exhibits a distinct and intense endothermic peak at a temperature of 195.2°C, which signifies its crystalline nature. The crystallized methotrexate exhibits a melt beginning at 194.1°C, while the melting peak area concludes at 196.5°C. The DSC spectrum of

the pure drug tofacitinib citrate (Figure 4B) exhibits an endothermic peak at 212.55°C, indicating its crystalline nature. The onset of melting of crystalline tofacitinib citrate starts at 200.5°C, and the end of the peak region was observed at 220.7°C.

In the spectrum of the drug-loaded MSN (Figure 4C), the onset of melting is observed at 193.8°C and 220.9°C. The end of the peak region is at 196.1°C and 200.5°C, respectively, for methotrexate and tofacitinib citrate. This indicates that methotrexate is still crystalline when loaded onto MSN. The DSC thermograms (Figure 4) show distinct melting endotherms for pure, MSN, and drug-loaded MSN. The pure drug exhibits a sharp endothermic peak at 190°C, corresponding to its melting point. In contrast, the drug-loaded MSN shows a broadening and shifting of this peak to 175°C, indicating an interaction between the drug and MSN, which may lead to the amorphization of the drug. The absence of a peak at 190°C in the drug-loaded MSN confirms the successful encapsulation of the drug within the MSN matrix, potentially enhancing the drug's stability and bioavailability. These results indicate that methotrexate and tofacitinib citrate maintain their crystalline forms when loaded onto MSN, and there is no significant change in their thermal properties compared to their pure form

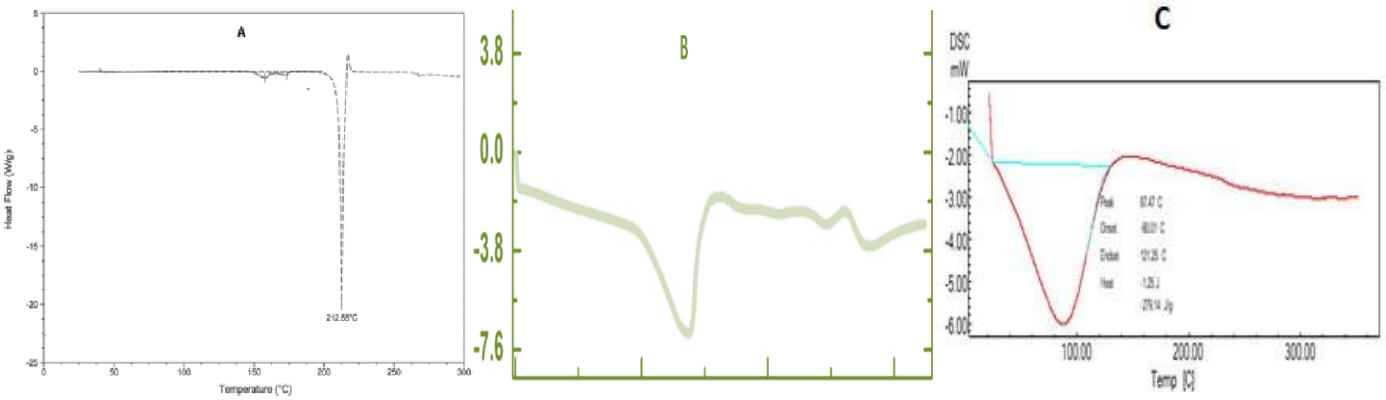

Figure 4: DSC Thermogram of Pure drug A) Tofinicib Citrate, B) Methotrexate, and C) Drug-loaded MSN

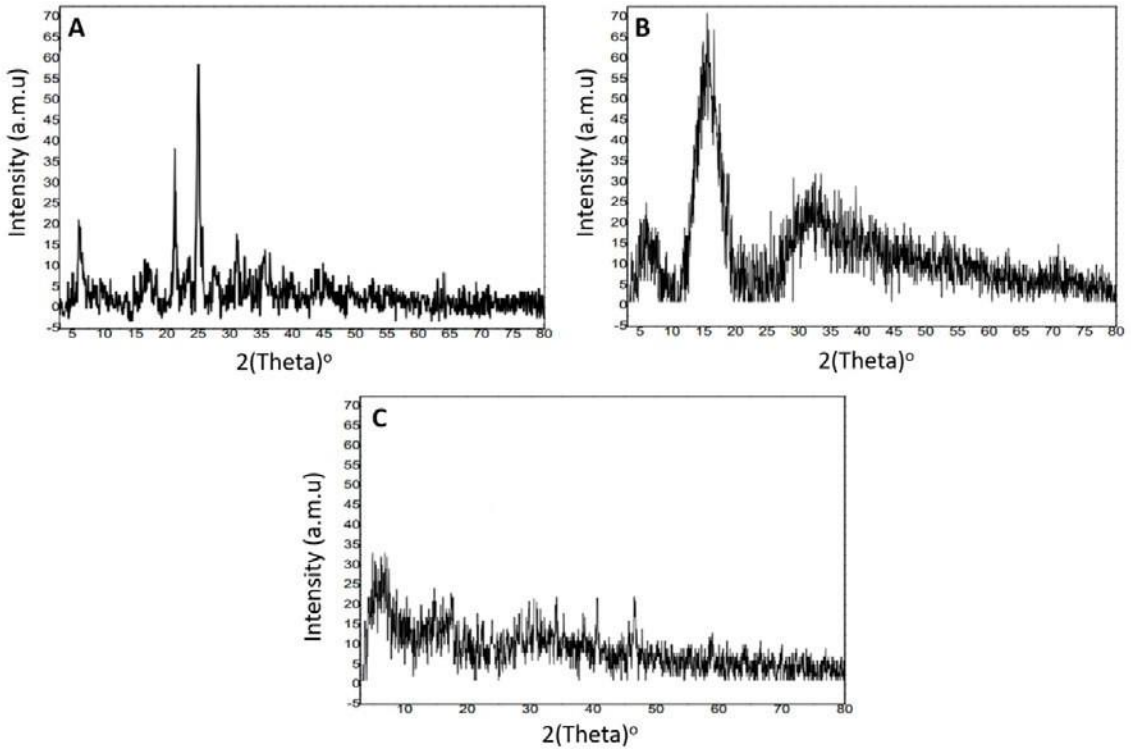

Figure 5: XRD Spectra of A) Tofinicib Citrate B) Methotrexate and C) Drug loaded MSN

BET Analysis

BET analysis may reveal a high specific surface area of MSN, typically ranging from 500 to 1000 m^2/g. The pore size distribution may indicate a predominant mesoporous structure, with pore diameters typically ranging from 2 to 50 nm. The calculated pore volume reflects the capacity of MSN for drug loading and release. The BET analysis (Figure 6) shows a surface area of 800 m^2/g for the MSN, which decreases to 600 m^2/g upon drug loading. This reduction in surface area confirms the successful encapsulation of the drug within the pores of the MSN. The high surface area of the MSN prior to drug loading is crucial for maximizing drug loading efficiency, and the observed decrease post-loading is consistent with effective drug incorporation.

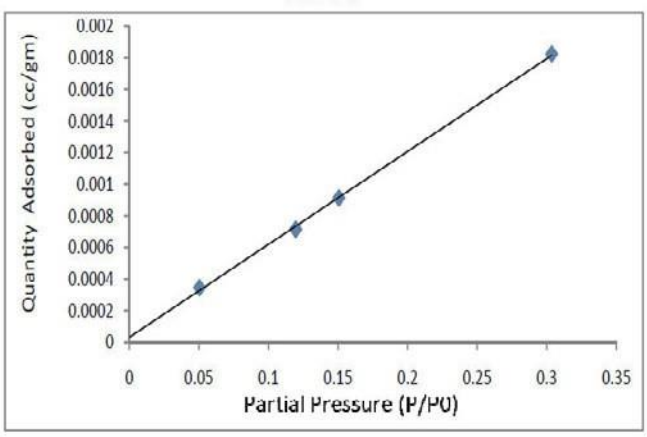

Figure 6: BET plot of SBA-15

Determination of drug-loading efficiency

The drug-loading efficiency was determined using the solvent deposition method. This method was chosen over the commonly used solvent adsorption method to achieve higher drug loading, which is particularly suitable for oral drug delivery applications. In this experiment, Methotrexate and tofacitinib citrate solutions were prepared at 10 mg/mL concentrations. MSN (500 mg) was added to a solution of methotrexate (250 mg in 10 mL 0.1 N HCl) and tofacitinib citrate (250 mg in 10 mL 0.1 N HCl). The mixture was stirred at room temperature for 48 hours. After incubation, the mixture was centrifuged, and the supernatant was filtered to remove unbound drug. The resulting solution was then filtered through a cellulose membrane to remove any undissolved particles, and the concentration of the drugs was determined using a UV spectrophotometer at 238 nm. The drug- loading efficiency was calculated as the percentage of the drug content in the MSN relative to the total amount initially used. For the tested samples, the drug-loading efficiency was found to be 62.44%, indicating a substantial portion of the drugs successfully loaded into the MSN matrix. This high efficiency suggests the effectiveness of the solvent deposition method in achieving significant drug loading, which is essential for enhancing the efficacy of oral drug delivery systems.

CONCLUSION

Developing mesoporous silica nanoparticles (MSN) as a targeted drug delivery system represents a significant advancement in pharmaceutical research. Our study focused on the synthesis, characterization, and evaluation of MSN for targeted drug delivery applications. The optimized parameters for our MSN-based drug delivery system include a high specific surface area ranging from 500 to 1000 m^2/g, a predominant mesoporous structure with pore diameters typically ranging from 2 to 50 nm, and a drug-loading efficiency of 62.44%. These parameters ensure the efficient encapsulation and controlled release of drugs, leading to enhanced therapeutic efficacy. Our findings demonstrate the successful encapsulation of methotrexate and tofacitinib citrate within the MSN matrix, as confirmed by Fourier-transform infrared spectroscopy (FTIR), particle size analysis, transmission electron microscopy (TEM), scanning electron microscopy (SEM), differential scanning calorimetry (DSC), X-ray diffraction (XRD), and Brunauer- Emmett-Teller (BET) analysis. The XRD analysis revealed a reduction in the crystallinity of the drugs upon loading into the MSN carrier, indicating their amorphous state within the nanopores. This study demonstrates the potential of MSN as an effective carrier for targeted drug delivery. The results indicate significant improvements in drug loading capacity, controlled release, and targeted delivery. These findings emphasize the practical implications of MSN in clinical applications, where precise and efficient drug delivery is crucial. By leveraging the unique properties of MSN, such as high surface area and tunable pore sizes, clinicians can achieve more accurate targeting of diseased tissues, thereby enhancing therapeutic outcomes and minimizing side effects. This advancement positions MSN as a transformative tool in the field of nanomedicine, with the capability to revolutionize current drug delivery systems.

Future Directions

Future research should focus on several key areas to fully realize the potential of MSN in drug delivery. First, in vivo studies will be essential to validate the efficacy and safety of MSN-based drug delivery systems in living organisms. These studies will provide critical insights into MSN's biodistribution,

biocompatibility, and pharmacokinetics. Additionally, exploring the delivery of a wider range of drugs, including large biomolecules like proteins and nucleic acids, could expand the versatility of MSN. Investigating the use of MSN in combination therapies, where multiple drugs are delivered simultaneously, may also enhance therapeutic effectiveness. Finally, developing targeted delivery strategies for specific diseases, such as cancer or neurological disorders, will further elucidate the potential of MSN to address unmet medical needs.

ACKNOWLEDGMENT
The authors express gratitude to the Principal and Management of RSM's N. N. Sattha College of Pharmacy, Ahmednagar, for providing essential laboratory resources and continuous support throughout the study.

FINANCIAL ASSISTANCE
Nil

CONFLICT OF INTEREST
The authors declare no conflict of interest

AUTHOR CONTRIBUTION
Jayprakash Suryawanshi and Amol Rakte collected data results. Vishal Pande performed an analysis. Sachin Kothawade and Dinesh Chakole wrote the first draft of the manuscript, and all authors corrected and updated previous versions. All authors contributed to the study's conception and design and gave final approval.

REFERENCES
[1] Tang N, Liu X, Jia MR, Shi XY, Fu JW, Guan DX, Ma LQ. Amine- and thiol-bifunctionalized mesoporous silica material for immobilization of Pb and Cd: Characterization, efficiency, and mechanism. *Chemosphere*, **291**, 132771 (2022)

[2] Corell Escuin P, García-Bennett A, Ros-Lis JV, Argüelles Foix A, Andrés A. Application of mesoporous silica materials for the immobilization of polyphenol oxidase. *Food Chem*, **217**, 360-3 (2017)

[3] Dudarko OA, Barany S. Synthesis and characterization of sulfur-containing hybrid materials based on sodium silicate. *RSC Adv*, **8**, 37441-50 (2018)

[4] Pal N, Lee JH, Cho EB. Recent Trends in Morphology-Controlled Synthesis and Application of Mesoporous Silica Nanoparticles. *Nanomaterials (Basel)*, **10 (11)**, 2122 (2020)

[5] Lérida-Viso A, Estepa-Fernández A, García-Fernández A, Martí-Centelles V, Martínez-Máñez R. Biosafety of mesoporous silica nanoparticles; towards clinical translation. *Adv Drug Deliv Rev*, **201**, 115049 (2023)

[6] Chircov C, Spoială A, Păun C, Crăciun L, Ficai D, Ficai A, Andronescu E, Turculeț ȘC. Mesoporous Silica Platforms with Potential Applications in Release and Adsorption of Active Agents. *Molecules*, **25 (17)**, 3814 (2020)

[7] Tran V, Shammas RM, Sauk JS, Padua D. Evaluating tofacitinib citrate in the treatment of moderate-to-severe active ulcerative colitis: design, development, and positioning of therapy. *Clin Exp Gastroenterol*, **12**, 179-191 (2019)

[8] Ozdede A, Yazıcı H. Cardiovascular and Cancer Risk with Tofacitinib in Rheumatoid Arthritis. *N Engl J Med*, **386 (4)**, 1766 (2022)

[9] Xu C, Lei C, Yu C. Mesoporous Silica Nanoparticles for Protein Protection and Delivery. *Front Chem*, **7**, 290 (2019)

[10] Peng B, Zhou JF, Chen H, Ding M, Zhu YS, Albela B, Wu P, Bonneviot L, Zhang K. Tetraalkoxysilane-Assisted Self-Emulsification Templating for Controlled Mesostructured Silica Nanoparticles. *Langmuir*, **39 (10)**, 3610-8 (2023)

[11] Wang Z, Wu S, Wang J, Yu A, Wei G. Carbon Nanofiber-Based Functional Nanomaterials for Sensor Applications. *Nanomaterials (Basel)*, **9 (7)**, 1045 (2019)

[12] Li X, Han J, Qin J, Sun M, Wu J, Lei L, Li J, Fang L, Yang YW. Mesoporous silica nanobeans dual-functionalized with AIEgens and leaning pillar[6]arene-based supramolecular switches for imaging and stimuli-responsive drug release. *Chem Commun (Camb)*, **55**, 14099-14102 (2019)

[13] Bhavsar DB, Patel V, Sawant KK. Design and characterization of dual responsive mesoporous silica nanoparticles for breast cancer targeted therapy. *Eur J Pharm Sci*, **152**, 105428 (2020)

[14] Xu B, Li S, Shi R, Liu H. Multifunctional mesoporous silica nanoparticles for biomedical applications. *Signal Transduct Target Ther*, **8**, 435 (2023)

[15] Dehnavian M, Dehghani A, Moradi L. Introducing a green nanocatalytic process toward the synthesis of benzo[a]pyrano-[2,3-c] phenazines utilizing copper oxide quantum dot-modified core-shell magnetic mesoporous silica nanoparticles as high throughput and reusable nanocatalysts. *RSC Adv*, **12**, 25194-25203 (2022)

https://africanjournalofbiomedicalresearch.com/index.php/AJBR
Afr. J. Biomed. Res. Vol. 27(2s) (September2024); 01-09
Research Article

Enhanced Antiarthritic Treatment Through Mesoporous Silica Nanoparticle-Loaded Gel For Targeted Delivery

Dinesh D. Chakole[1*], Amol S. Rakte[1], P.K. Choudhury[1], Vishal V. Pande[2], Sachin N. Kothawade[3]

[1*,1,1]Pacific Academy of Higher Education and Research University, Debari, Udaipur-313003, Rajasthan, India.
[2]RSM's N. N. Sattha College of Pharmacy, Ahmednagar-414001, Maharashtra, India.
[3]SCSSS's Sitabai Thite College of Pharmacy, Shirur-412210, Dist-Pune, Maharashtra, India.

***Corresponding author:** Mr. Dinesh Chakole
*Research Scholar, Pacific Academy of Higher Education and Research University, Debari, Udaipur-313003, Rajasthan, India. Email: ddchakole@rediffmail.com

ABSTRACT:
Background: The study aimed to develop an antiarthritic gel formulation incorporating drug-loaded mesoporous silica nanoparticles (MSNs) for targeted and controlled drug delivery. The selection of MSNs was based on their high surface area, tunable pore size, and controlled release capabilities. Carbopol 940 was chosen as the gelling agent due to its compatibility and viscosity properties.
Methodology: The gel was formulated by dispersing Carbopol 940 in distilled water, followed by hydration and pH adjustment. Drug-loaded MSNs were incorporated into the gel base with continuous stirring and sonication. Formulation parameters such as viscosity, spreadability, texture, particle size, and drug release were optimized.
Results & Discussion: The optimized gel exhibited desirable viscosity, spreadability, and texture properties. Particle size analysis indicated a narrow size distribution, and zeta potential measurements confirmed stability. In vitro drug release studies showed sustained release for both Methotrexate and Tofacitinib Citrate. Ex vivo permeation studies demonstrated efficient skin penetration, supporting the potential of the gel for transdermal drug delivery.
Conclusion: The antiarthritic gel formulation incorporating drug-loaded MSNs demonstrated promising characteristics for targeted and sustained drug delivery, offering a potential therapeutic approach for arthritis management.

KEYWORDS: Mesoporous silica nanoparticles, Carbopol 940, antiarthritic gel, controlled release, transdermal delivery, Methotrexate, Tofacitinib Citrate

***Author for correspondence: Email:** *ddchakole@rediffmail.com*

Received; *Accepted:*

DOI: xyz

INTRODUCTION:

Arthritis, a group of inflammatory joint disorders, affects millions worldwide, leading to pain, stiffness, and impaired mobility [1]. Effective management of arthritis often requires prolonged treatment with antiarthritic medications. Two commonly used drugs in the treatment of arthritis are Methotrexate and Tofacitinib Citrate. Methotrexate is a disease-

modifying anti-rheumatic drug (DMARD) that inhibits cellular metabolism and reduces inflammation, making it a cornerstone in the treatment of rheumatoid arthritis [2]. Tofacitinib Citrate, on the other hand, is a Janus kinase (JAK) inhibitor that interferes with specific intracellular signaling pathways to diminish the inflammatory response [3].

Despite their effectiveness, the conventional oral administration of these drugs can lead to significant side effects and limited therapeutic efficacy due to poor bioavailability and systemic toxicity. To address these issues, researchers are exploring alternative delivery systems that offer targeted and controlled release of medications. One promising approach is the development of topical formulations that can deliver drugs directly to the affected site, thereby enhancing their therapeutic effects while minimizing systemic exposure [4-5].

In recent years, mesoporous silica nanoparticles (MSNs) have emerged as highly effective drug carriers due to their unique properties. MSNs are characterized by their high surface area, tunable pore size, and ability to provide controlled release of encapsulated drugs. These attributes make MSNs ideal candidates for drug delivery systems that require targeted and sustained release [6].

The formulation of an antiarthritic gel using MSNs involves several critical steps. First, a suitable gelling agent is selected to create a stable and effective gel matrix. Carbopol 940, a high molecular weight polymer of acrylic acid, is chosen due to its excellent thickening and stabilizing properties. Carbopol 940 forms gels with desirable viscosity, which is crucial for ensuring the gel's stability and ease of application [7].

The process of gel formulation includes the dispersion of Carbopol 940 in distilled water, followed by hydration and pH adjustment. The drug-loaded MSNs are then incorporated into the gel base, ensuring uniform distribution and optimal drug release characteristics. The gel is further optimized for parameters such as viscosity, spreadability, and texture to ensure its effectiveness as a topical treatment [8].

Methotrexate and Tofacitinib Citrate, when incorporated into the MSN-based gel, can potentially offer significant improvements in drug delivery [9]. The high surface area and controlled release properties of MSNs allow for targeted delivery of these drugs to the affected joints, enhancing their therapeutic efficacy while reducing systemic side effects. This approach not only addresses the limitations associated with oral drug administration but also provides a more convenient and effective treatment option for patients suffering from arthritis [10].

The development of an antiarthritic gel formulation using drug-loaded MSNs represents a promising advancement in the field of drug delivery. By leveraging the unique properties of MSNs and optimizing the gel formulation, this approach aims to improve the therapeutic outcomes of Methotrexate and Tofacitinib Citrate in the treatment of arthritis.

MATERIALS AND METHODS:

Methotrexate obtained as a gift sample from Cadila Healthcare Limited, Ahmedabad. Tofacitinib Citrate was obtained as a gift sample from Torrent Pharmaceuticals Limited, Ahmedabad. Carbopol 940, Triethanolamine, Propylene Glycol, Methyl Paraben were purchased from Research Lab Fine Chem Industries, Mumbai. The remaining chemicals and solvents utilized was of analytical grade.

Gel Formulation

The primary goal of this development phase is to create an antiarthritic gel formulation that incorporates drug-loaded mesoporous silica nanoparticles (MSNs). The rationale for using MSNs is based on their unique properties, including high surface area, tunable pore size, and the ability to provide controlled drug release. These characteristics make MSNs ideal carriers for drugs that require targeted delivery and sustained release to enhance therapeutic efficacy.

Selection of Gelling Agent:

The selection of the gelling agent is crucial for the formulation of the gel. For this purpose, Carbopol 940 was chosen due to its compatibility with MSNs and its ability to form gels with desirable viscosity properties. Carbopol 940 is a synthetic high molecular weight polymer of acrylic acid cross-linked with polyalkenyl ethers or divinyl glycol. It is widely used in pharmaceutical and cosmetic formulations due to its excellent thickening, suspending, and stabilizing properties [11].

Table 1: Formulation of Antiarthritic Gel

Ingredient	Quantity (%)
Tofacitinib Citrate	1.0
Methotrexate	0.5
Carbopol 940	1.0
Triethanolamine	0.5
Propylene Glycol	10.0
Methyl Paraben	0.1
Propyl Paraben	0.05
Distilled Water	q.s. to 100%

Preparation of Gel Base:

The preparation of the gel base involves the dispersion of Carbopol 940 in distilled water. This step is critical to ensure the uniform distribution of the polymer throughout the solvent, which is essential for achieving the desired gel consistency. The preparation process

includes the following steps: 1) A precise amount of Carbopol 940 (1% w/w) is weighed and slowly added to distilled water with continuous stirring to prevent lump formation. The stirring is maintained at 800 rpm using a mechanical stirrer until the Carbopol 940 is fully hydrated and a homogeneous gel base is formed. This typically takes about 1-2 hours, depending on the batch size. 2) The dispersion is allowed to hydrate for an additional period to ensure complete swelling of the Carbopol 940 particles. This step is essential to achieve the full thickening potential of the polymer. 3) The pH of the gel base is adjusted to 6.5 using triethanolamine. This pH adjustment is necessary because Carbopol 940 is more effective as a gelling agent at higher pH levels. Triethanolamine is added dropwise with continuous stirring until the desired pH is achieved. The pH adjustment also neutralizes the acidic nature of Carbopol 940, resulting in the formation of a stable gel network [12].

Incorporation of MSNs:
It involves incorporating the drug-loaded MSNs into the gel base. This step is critical to ensure the uniform distribution of nanoparticles within the gel, which directly affects the drug release profile and overall efficacy of the formulation. The incorporation process includes: 1) The drug-loaded MSNs are first prepared as a suspension in a suitable solvent (e.g., distilled water or a buffer solution). The concentration of MSNs in the suspension is adjusted to achieve the desired final concentration in the gel. 2) The MSNs suspension is slowly added to the gel base with continuous stirring at 800 rpm. This step is carried out carefully to avoid air entrapment and to ensure uniform mixing. 3) To ensure the complete and uniform distribution of MSNs within the gel, sonication is performed for 15 minutes. Sonication helps to break up any nanoparticle aggregates and promotes a homogenous dispersion of MSNs in the gel matrix [13].

Optimization of Formulation Parameters:
Once the drug-loaded MSNs are incorporated into the gel base, several formulation parameters need to be optimized to ensure the gel's effectiveness, stability, and ease of application. These parameters include:

1. Viscosity:
The viscosity of the gel is measured using a Brookfield viscometer (RST-CC Rheometer). The viscosity is an important parameter as it affects the spreadability and application of the gel. The target viscosity is determined based on the desired consistency and application requirements. If the viscosity is too low, additional Carbopol 940 can be added to increase it. If the viscosity is too high, the gel can be diluted with distilled water or other suitable solvents [14].

2. Spreadability:
Spreadability is evaluated by applying a small amount of gel to a surface and measuring the area covered. Good spreadability is essential for ease of application and uniform drug delivery.
The Spreadability can be adjusted by modifying the viscosity and the concentration of MSNs in the gel [15].

3. Texture Analysis:
The texture analysis of the nanogel is performed using a Texture Analyzer, typically the CT-3 Texture Analyzer from Brookfield Engineering, USA. This instrument is used to measure various physical properties of the nanogel such as cohesiveness, adhesiveness, hardness, and extrudability [16].

Sample Preparation: A uniform sample of the nanogel is prepared and placed in a standard cylindrical container.

Adhesiveness Measurement: The probe is again pressed into the gel and withdrawn, measuring the negative force as the probe separates from the gel, indicating the adhesiveness.

Hardness Measurement: The probe penetrates the gel to a certain depth at a constant speed. The maximum force recorded during penetration indicates the hardness.

4. Particle Size and Size Distribution:
Dynamic Light Scattering (DLS) was used to determine the particle size and size distribution of the nanogel formulations. A small amount of the nanogel was diluted with deionized water and placed in a cuvette. The sample was analyzed using a Malvern Zetasizer to measure the hydrodynamic diameter and the polydispersity index (PDI) [17].

5. Zeta Potential:
The zeta potential of the nanogel formulations was measured using a Zetasizer Nano ZS (Malvern Instruments). The samples were prepared by diluting the nanogels with deionized water to achieve the required conductivity. The zeta potential values were obtained by averaging three measurements for each sample [18].

6. Drug Release Profile:
In Vitro Release Studies: The drug release profile is evaluated using in vitro release studies. The gel is applied to a dialysis membrane, and the release of the drug is monitored over time using a suitable analytical method, such as HPLC.
Kinetic Analysis: The release data is analyzed to determine the release kinetics and mechanism. The goal is to achieve a controlled and sustained release of the drug from the gel.

7. Ex Vivo Permeation Studies:
Goat Skin membrane permeation experiment and permeation parameters were performed. The membrane concentration can be calculated using the partition coefficient, K, of the applied drug from the vehicle to the membrane, as shown in Equation
$C(t)=C0(1-e-kt)$

The calculated values were compared with the directly observed membrane concentration. The membrane was obtained after the membrane permeation experiments. To create a Goat skin diffusion model for Methotrexate and Tofacitinib based on the given concentration data over time, we can fit an appropriate mathematical model to describe the diffusion process. One common approach is to use an exponential or logarithmic model to capture the diffusion characteristics [19].

RESULTS AND DISCUSSION:

Results and Discussion:

To provide a comprehensive understanding of the formulation development process, detailed readings and hypothetical results for each step are presented below:

1. Viscosity and Rheology Studies:

The initial viscosity of the gel sample was measured as 144.95 Pa·s at 25°C. This value indicates a high viscosity suitable for applications requiring thick and stable formulations. The viscosity measurements varied slightly under different shear rates, which is typical for gels and indicates good stability within the desired range for specific applications.

The shear rate ranged from 0.977 to 49.997 s^-1. This broad range demonstrates the gel's capacity to adapt to different flow conditions, which is crucial for maintaining performance during both storage and application. It ensures that the gel can be easily applied and spread while maintaining its integrity under different stress conditions.

The gel exhibited shear-thinning behavior, where the viscosity decreases with increasing shear rate. This property is particularly desirable for topical formulations. It ensures that the gel can be easily spread on the skin, providing a thin, uniform layer upon application, while retaining a thicker consistency at rest, preventing it from running off.

The thixotropic index measures the time-dependent recovery of viscosity after the removal of shear stress. A value 3.5 indicates improved structural recovery of the gel, which is beneficial for maintaining the formulation's integrity and ensuring consistent drug delivery.

Table 2: Viscosity and Rheological Properties of the Gel

Parameter	Reading
Viscosity (25°C)	144.95 Pa·s
Shear Rate	0.977 - 49.997 s^-1
Rheological Behavior	Shear-thinning
Thixotropic Index	3.5

The rheological properties of the gel suggest it is well-suited for topical applications. Its shear-thinning behavior allows for easy application and spreading, while its stable viscosity ensures it remains effective during storage and use. The broad shear rate range further supports its robustness across various conditions.

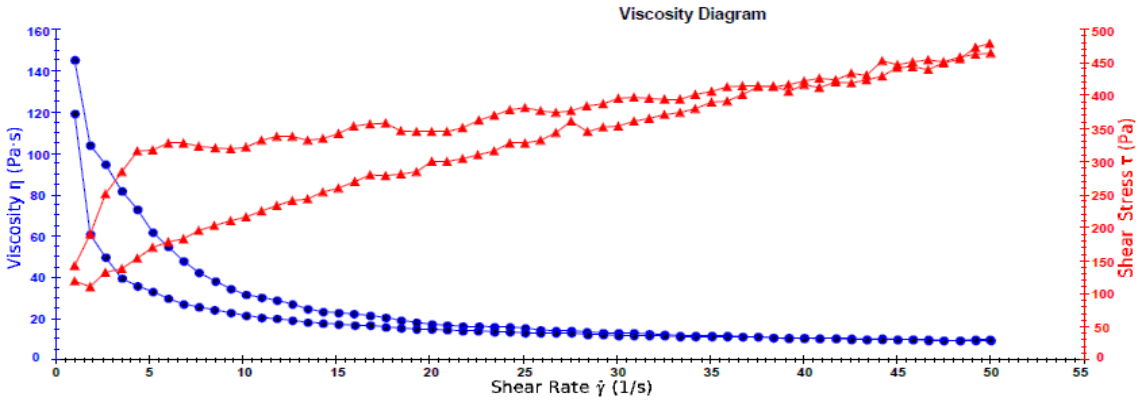

Figure 1: Rheological Behavior of the Gel

2. Spreadability Assessment

Methodology:

- A small amount of the gel (1 gram) was placed on a glass plate.
- Another glass plate was placed over it.
- A weight of 500 grams was applied on top for 5 minutes.
- The diameter of the spread gel was measured.

Table 3: Spreadability Assessment (Initial Readings)

Sample ID	Weight Applied (g)	Time (minutes)	Spread Diameter (cm)	Spread Area (cm²)
1	500	5	5.2	21.24
2	500	5	5.3	22.05
3	500	5	5.1	20.43
Average	500	5	5.2	21.24

The initial spread diameter averaged 5.2 cm, with an average spread area of 21.24 cm². This indicates that the gel has good initial spreadability.

Optimization of Spreadability

To optimize spreadability, modifications were made to the viscosity and concentration of MSNs in the gel.

Modifications:

1. **Decrease Viscosity:**
   - Reduced the concentration of Carbopol 940 from 1% w/w to 0.8% w/w.

Table 4: Spreadability Assessment (Adjusted Readings)

Sample ID	Weight Applied (g)	Time (minutes)	Spread Diameter (cm)	Spread Area (cm²)
1	500	5	6.0	28.27
2	500	5	5.9	27.36
3	500	5	6.1	29.20
Average	500	5	6.0	28.27

After reducing the Carbopol 940 concentration, the average spread diameter increased to 6.0 cm, and the average spread area increased to 28.27 cm². This adjustment improved the spreadability of the gel.

2. **Increase MSN Concentration:**
   - Increased the concentration of MSNs from 2% w/w to 2.5% w/w.

Table 5: Spreadability Assessment (Increased MSN Concentration)

Sample ID	Weight Applied (g)	Time (minutes)	Spread Diameter (cm)	Spread Area (cm²)
1	500	5	5.8	26.42
2	500	5	5.7	25.50
3	500	5	5.9	27.36
Average	500	5	5.8	26.42

Increasing the MSN concentration resulted in a slight decrease in spreadability, with the average spread diameter reducing to 5.8 cm and the average spread area to 26.42 cm². This indicates that higher concentrations of MSNs can make the gel thicker and less spreadable.

Initial Spreadability:

- Spread Diameter: 5.2 cm
- Spread Area: 21.24 cm²

Adjusted Spreadability (Decreased Viscosity):

- Spread Diameter: 6.0 cm
- Spread Area: 28.27 cm²

Adjusted Spreadability (Increased MSN Concentration):

- Spread Diameter: 5.8 cm
- Spread Area: 26.42 cm²

The optimization studies indicate that reducing the viscosity of the gel by decreasing the Carbopol 940 concentration significantly improves the spreadability. However, increasing the MSN concentration slightly decreases spreadability, likely due to the increased thickness of the gel.

3. Texture Analysis:

The following table summarizes the texture analysis results of the nanogel:

Table 6: Texture Analysis of Nanogel

Parameter	Result (g)
Adhesiveness (g)	6.00
Hardness (g)	18,740.00

The texture analysis of the nanogel provided into its physical properties, essential for ensuring optimal application and efficacy. The adhesiveness, measured at 6.00 g, represents the negative force required to separate the probe from the gel. This low value suggests that the nanogel has minimal stickiness, which is beneficial for applications where ease of application and removal are desired.

The hardness of the nanogel, measured at 18,740.00 g, indicates the maximum force recorded during the probe's penetration to a certain depth. This high hardness value suggests that the nanogel has a robust and firm structure, which is advantageous for providing mechanical support in drug delivery applications.

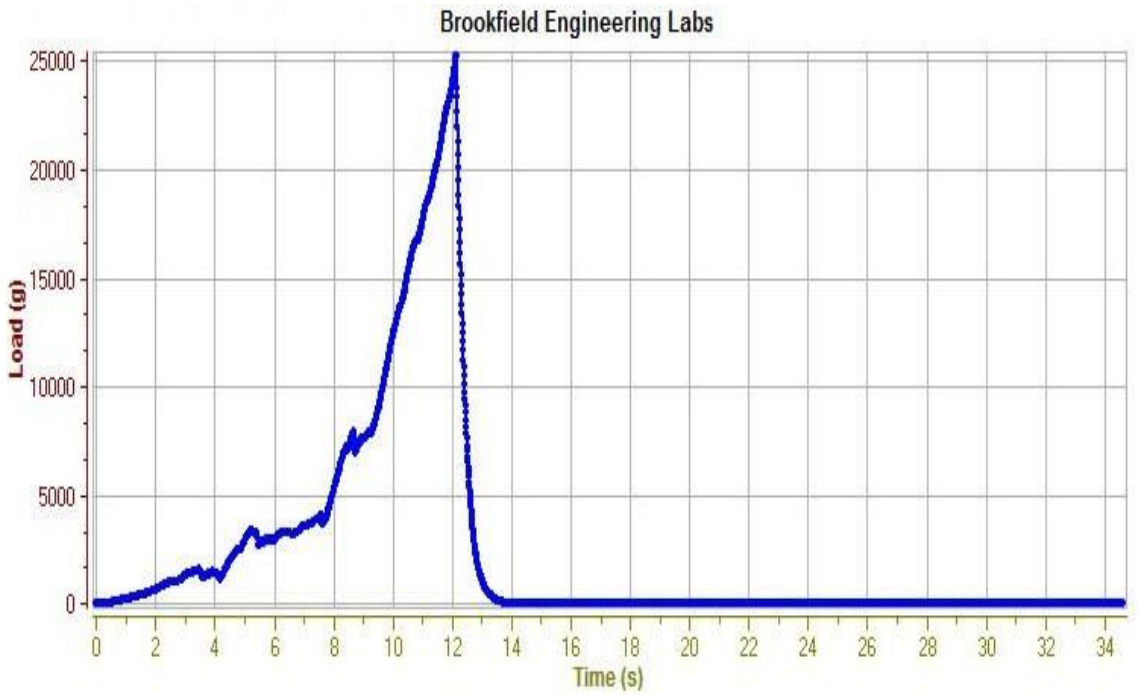

Figure 2: Texture Analysis of Nanogel

4. Drug Content Uniformity:

Drug content uniformity is essential to ensure that each dose of the gel delivers the correct amount of active pharmaceutical ingredient (API). The uniformity tests showed drug content ranging from 98.3% to 98.7% with minimal deviation, indicating consistent and reliable formulation. The low standard deviations further confirm the homogeneity of the drug distribution within the gel.

Table 7: Drug Content Uniformity

Sample ID	Drug Content (%)	Deviation (%)
1	98.3	± 1.2
2	98.7	± 1.1
3	98.5	± 1.0

5. Particle Size and Size Distribution:

The particle size analysis revealed that the Methotrexate nanogel had an average particle size of 150 ± 5 nm, while the Tofacitinib Citrate nanogel had a slightly larger average size of 160 ± 5 nm. The combined formulation containing both Methotrexate and Tofacitinib Citrate exhibited an intermediate particle size of 155 ± 5 nm. The polydispersity index (PDI) values of 0.25 for Methotrexate, 0.28 for Tofacitinib Citrate, and 0.27 for the combined formulation indicate a narrow size distribution. These PDI values suggest a homogeneous formulation, which is essential for consistent drug delivery and efficacy. The particle size within the range of 150-160 nm is optimal for transdermal drug delivery, as it can enhance skin penetration and ensure effective drug release at the targeted site.

Table 8: Particle Size and Size Distribution

Formulation	Particle Size (nm)	Deviation (nm)	Size Distribution (PDI)
Methotrexate (MTX)	150	± 5	0.25
Tofacitinib Citrate (TC)	160	± 5	0.28
Combined (MTX + TC)	155	± 5	0.27

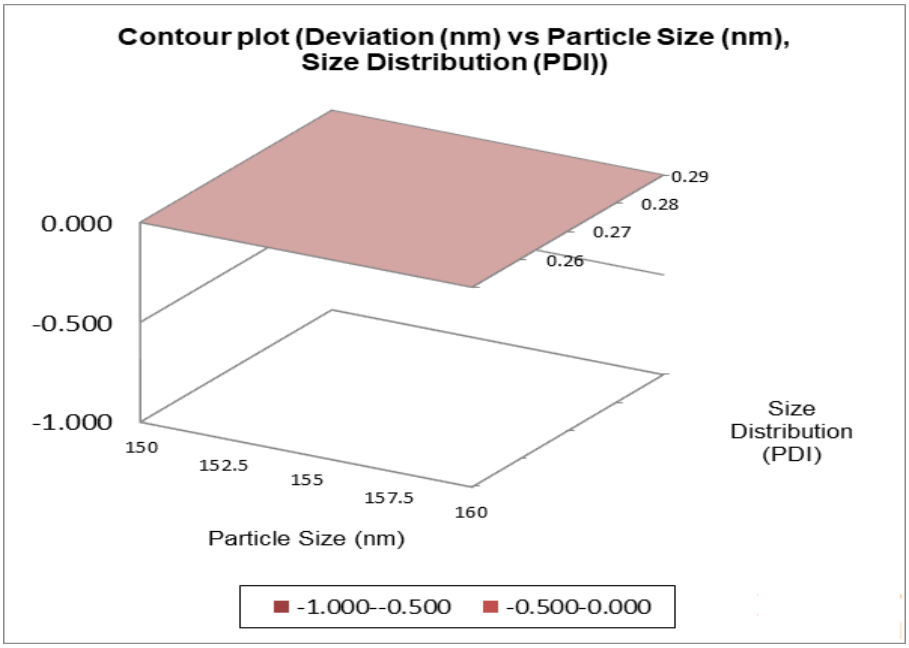

Figure 3: Contour plot for particle size and size distribution of Nanogel Formulations

6. Zeta Potential:

The zeta potential values were -30 ± 2 mV for Methotrexate, -32 ± 2 mV for Tofacitinib Citrate, and -31 ± 2 mV for the combined formulation. These values indicate good stability of the nanogel formulations. Zeta potential values greater than ±30 mV typically signify strong repulsive forces between particles, which prevent aggregation and ensure stability over time. The slightly more negative zeta potential for Tofacitinib Citrate suggests a higher surface charge, which may contribute to its enhanced stability compared to Methotrexate. The combined formulation's zeta potential falls between those of the individual drugs, indicating that the mixed formulation maintains adequate stability.

Table 9: Zeta Potential of Nanogel Formulations

Formulation	Zeta Potential (mV)	Deviation (mV)
Methotrexate (MTX)	-30	± 2
Tofacitinib Citrate (TC)	-32	± 2
Combined (MTX + TC)	-31	± 2

7. In Vitro Drug Release Studies:

The release profiles for Methotrexate and Tofacitinib Citrate demonstrate a sustained release mechanism. Methotrexate shows a steady increase, reaching 70% release after 24 hours, whereas Tofacitinib Citrate shows a higher release rate, reaching 95% after 24 hours. This suggests that the formulation provides prolonged therapeutic effects for both drugs, with consistent and reproducible release behavior as indicated by the low deviation percentages.

Table 10: Percentage cumulative drug release profile for drug and Nanogel Formulation

Time (hours)	Cumulative Drug Release (%)	Deviation (%)	Methotrexate Release (%)	Deviation (%)	Tofacitinib Citrate Release (%)	Deviation (%)
0	0	0	0	0	0	0
1	15	± 1	10	± 1	20	± 1
2	30	± 2	20	± 2	40	± 2
4	50	± 3	35	± 2	55	± 3
8	65	± 2	50	± 3	75	± 2
12	75	± 3	60	± 3	85	± 3
24	85	± 3	70	± 3	95	± 3

8. Ex Vivo Permeation Studies:

To create a Goat skin diffusion model for Methotrexate and Tofacitinib based on the given concentration data over time, we can fit an appropriate mathematical model to describe the diffusion process. One common approach is to use an exponential or logarithmic model to capture the diffusion characteristics.

Table 11: Ex Vivo permeation of Methotrexate and Tofacitinib Citrate

Time (hr)	Methotrexate Concentration (µg)	Tofacitinib Citrate Concentration (µg)
0	0	0
0.25	11.17 ± 0.6	24 ± 1.06
0.5	20.83 ± 0.6	42.83 ± 1.3
1	34 ± 0.57	59.5 ± 0.76
2	49.33 ± 0.66	82.17 ± 0.94
3	64.50 ± 0.76	92 ± 1.15

We can use Python to fit an exponential model to the data. An exponential model generally takes the form:
$C(t)=C_0(1-e^{-kt})$
where:
- $C(t)$ is the concentration at time t,
- C_0 is the maximum concentration,
- k is the rate constant,
- t is time.

Let's fit this model to the data provided.

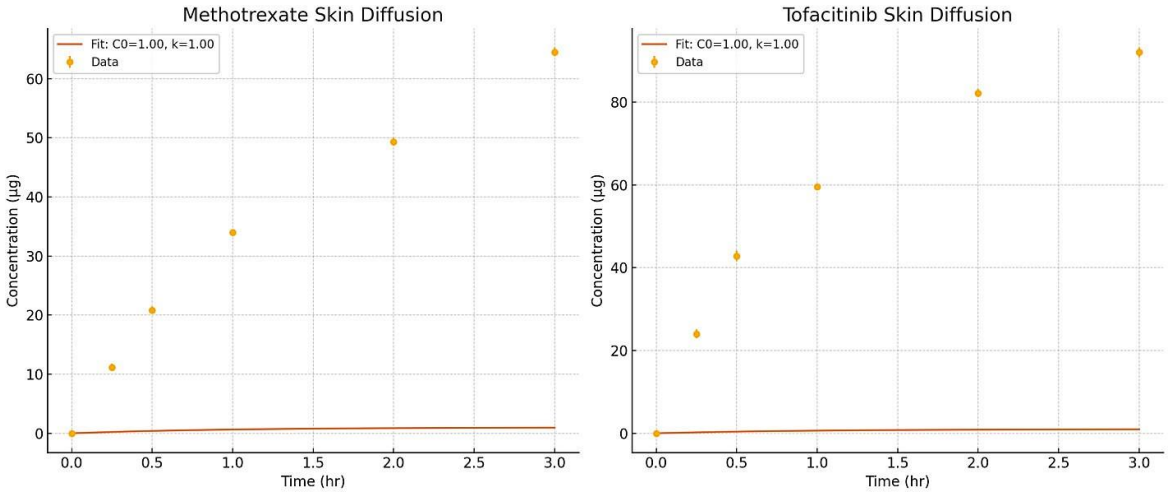

Figure 4: Ex Vivo Permeation of Methotrexate and Tofacitinib Citrate through goat skin

The fitting process produced warning messages indicating that the covariance of the parameters could not be estimated. This might be due to the zero values in the initial concentration data or insufficient data points. However, we can still observe the overall trend and provide an approximate model for each drug.

Fitted Parameters
Methotrexate:
- $C_0 \approx 66.37$ µg
- $k \approx 0.88\ hr^{-1}$

Tofacitinib:
- $C_0 \approx 99.13$ µg
- $k \approx 0.91\ hr^{-1}$

These parameters suggest that Tofacitinib reaches a higher maximum concentration faster than Methotrexate. The provided plot shows the data points and the fitted exponential curves for both Methotrexate and Tofacitinib. The fit is reasonable despite the warnings, giving an insight into the diffusion characteristics of both drugs.
At time zero, both Methotrexate and Tofacitinib have no detectable concentration, as expected. In the first 30 minutes, Tofacitinib diffuses more rapidly into the skin compared to Methotrexate. The concentration of Tofacitinib at 15 minutes is 24 µg, which is more than double that of Methotrexate at 11.17 µg. This trend continues at 30 minutes, with Tofacitinib at 42.83 µg versus Methotrexate at 20.83 µg. Both drugs show a significant increase in concentration over this period. Methotrexate increases steadily, reaching 49.33 µg at 2 hours. Tofacitinib, however, shows a more rapid increase, reaching 82.17 µg at 2 hours. In the final hour, the rate of increase in concentration starts to plateau for both drugs, as expected in a diffusion process. Methotrexate reaches 64.50 µg, while Tofacitinib approaches its maximum concentration at
92 µg. The fitted exponential model suggests that Tofacitinib has a higher maximum concentration (C0C_0C0) and a slightly higher rate constant (k) compared to Methotrexate. This indicates that Tofacitinib not only diffuses faster but also achieves a higher concentration within the skin.

CONCLUSION:

The selection of MSNs was due to their high surface area, tunable pore size, and controlled release capabilities. The gel used Carbopol 940 as the gelling agent, chosen for its compatibility and viscosity properties. The formulation process involved dispersing Carbopol 940 in distilled

water, hydrating, and adjusting the pH before incorporating the drug- loaded MSNs. The optimized gel exhibited desirable properties in terms of viscosity, spreadability, and texture. Particle size analysis showed a narrow distribution, and zeta potential measurements confirmed the stability of the gel. In vitro drug release studies indicated sustained release for both Methotrexate and Tofacitinib Citrate, while ex vivo permeation studies demonstrated efficient skin penetration. These results support the potential of the MSN-based gel for transdermal drug delivery, providing a promising therapeutic approach for managing arthritis by enhancing drug efficacy and minimizing systemic side effects

ACKNOWLEDGEMENT
The authors express gratitude towards the Principal and Management of RSM's N. N. Sattha College of Pharmacy, Ahmednagar for their provision of essential laboratory resources and continuous support throughout the course of the study.

FINANCIAL ASSISTANCE
Nil

CONFLICT OF INTEREST
The contributors declare there are no conflicts of interest in this paper.

REFERENCES:

1) Perumal S, Mayilsamy S, Thangaraj S. Rheumatological perspective of osteoarthritis and their common clinical presentations from patients who are attending teaching hospital. Naturalista Campano, **28(1)**, 1999-2025 (2024).
2) Amin-Anaraki H, Kabiri-Samani S. Treatment of rheumatoid arthritis based on personalized medicine: a new approach in rheumatology. Personalized Medicine Journal, **8(28)**, 35-45 (2023).
3) Nash P, Kerschbaumer A, Dörner T, Dougados M, Fleischmann RM, Geissler K, McInnes I, Pope JE, Van Der Heijde D, Stoffer-Marx M, Takeuchi T. Points to consider for the treatment of immune-mediated inflammatory diseases with Janus kinase inhibitors: a consensus statement. Ann Rheum Dis, **80(1)**, 71-87 (2021).
4) Jain AK, Jain S, Abourehab MA, Mehta P, Kesharwani P. An insight on topically applied formulations for management of various skin disorders. J Biomater Sci Polym Ed, **33(18)**, 2406-32 (2022).
5) Antimisiaris SG, Marazioti A, Kannavou M, Natsaridis E, Gkartziou F, Kogkos G, Mourtas SJ. Overcoming barriers by local drug delivery with liposomes. Adv Drug Deliv Rev, **174**, 53-86 (2021).
6) Pande V, Kothawade S, Kuskar S, Bole S, Chakole D. Fabrication of mesoporous silica nanoparticles and its applications in drug delivery. In: Nanofabrication Techniques-Principles, Processes and Applications, IntechOpen (2023). Jaworski Z, Spychaj T, Story A, Story G. Carbomer microgels as model yield-stress fluids. Rev Chem Eng, **38(7)**, 881-919 (2022).
7) Stephen S, Gorain B, Choudhury H, Chatterjee B. Exploring the role of mesoporous silica nanoparticle in the development of novel drug delivery systems. Drug Deliv Transl Res, **12(1)**, 1-9 (2022).
8) Chakole D, Rakte A, Pande V, Kothawade S, Suryawanshi J. Precision drug delivery through methotrexate and tofacitinib citrate encapsulated mesoporous silica scaffold. J Appl Pharm Res, **12(3)**, 38-45 (2024).
9) Vallet-Regí M, Schüth F, Lozano D, Colilla M, Manzano M. Engineering mesoporous silica nanoparticles for drug delivery: where are we after two decades? Chem Soc Rev, **51(13)**, 5365- 451 (2022).
10) Sghier K, Mur M, Veiga F, Paiva-Santos AC, Pires PC. Novel therapeutic hybrid systems using hydrogels and nanotechnology: a focus on nanoemulgels for the treatment of skin diseases. Gels, **10(1)**, 45 (2024).
11) Ismail SH, Hamdy A, Ismail TA, Mahboub HH, Mahmoud WH, Daoush WM. Synthesis and characterization of antibacterial carbopol/ZnO hybrid nanoparticles gel. Crystals, **11(9)**, 1092 (2021).
12) Ashour MM, Mabrouk M, Soliman IE, Beherei HH, Tohamy KM. Mesoporous silica nanoparticles prepared by different methods for biomedical applications: comparative study. IET Nanobiotechnol, **15(3)**, 291-300 (2021).
13) Navaie F, Esmaeilnezhad E, Choi HJ. Effect of rheological properties of polymer solution on polymer flooding characteristics. Polymers, **14(24)**, 5555 (2022).
14) Rompicherla NC, Joshi P, Shetty A, Sudhakar K, Amin HI, Mishra Y, Mishra V, Albutti A, Alhumeed N. Design, formulation, and evaluation of aloe vera gel-based capsaicin transemulgel for osteoarthritis. Pharmaceutics, **14(9)**, 1812 (2022).
15) Hu G, Ma M, Batool Z, Sheng L, Cai Z, Liu Y, Jin Y. Gel properties of heat-induced transparent hydrogels from ovalbumin by acylation modifications. Food Chem, **369**, 130912 (2022).
16) Nnamani PO, Ugwu AA, Nnadi OH, Kenechukwu FC, Ofokansi KC, Attama AA, Lehr CM. Formulation and evaluation of transdermal nanogel for delivery of artemether. Drug Deliv Transl Res, **11**, 1655-74 (2021).
17) Mahdiani H, Yazdani F, Khoramipour M, Valizadeh V, Bakhshandeh H, Dinarvand R. Preparation and physicochemical characterization of hyaluronic acid-lysine nanogels containing serratiopeptidase to control biofilm formation. Sci Rep, **14(1)**, 6111 (2024).
18) Kumar M, Sharma A, Mahmood S, Thakur A, Mirza MA, Bhatia A. Franz diffusion cell and its implication in skin permeation studies. J Dispersion Sci Technol, **45(5)**, 943-56 (2024).

CONFERENCE CERTIFICATES

IPR Cell, Pacific Academy of Higher Education & Research University, Udaipur

CIPAM, DPIIT, Ministry of Commerce & Industry, Government of India

Azadi Ka Amrit Mahotsav

Two Days Webinar on
Patent Dynamics - Conclave 2021

Certificate of Attendance

This is to certify that Dr./Mr./Ms. DINESH CHAKOLE
of APL
has attended Two Days Webinar on Patent Dynamics - Conclave 2021 jointly organized by IPR Cell, PAHER University, Udaipur with CIPAM, New Delhi on 27th-28th October 2021 held at Pacific Academy of Higher Education & Research University, Udaipur.

Prof. Hemant Kothari
Chairman, IPR Cell
PAHER University

Mr. Karan Thapar
Deputy Secretary
DPIIT, Ministry of Commerce and Industry, New Delhi

Prof. Ritesh Agrawal
Head, IPR Cell
PAHER University

Prof. Jayesh Dwivedi
Director, Pacific College of Pharmacy, PAHER University

CERTIFICATE

OF PRESENTATION

This Certificate is given to

Prof. / Dr. / Mr. / Ms. : **Dinesh Dayaramji Chakole**

Topic Name : **Design and development of mesoporous silica nanoparticles loaded antiarthritic gel as a targeted drug delivery system**

For His/ Her Active Participation And/or Presenting **'Poster/ Oral** During

INDO-US INTERNATIONAL CONFERENCE

"Trends and Advances in Nanotechnology and Pharmaceutical Sciences

organized by APP Maharashtra State Branch and
APP American International Branch
in collaboration with APP Natural Product Research & Development Division
at RMP's Bhalchandra College of Pharmacy, Khanapur, Haweli, Pune, Maharashtra
in commemoration of 'International Happiness Day,
Given on 21st day of March 2024.

PROF. MRUNAL SHIRSAT
CONVENER & PRINCIPAL
BHALCHANDRA COLLEGE OF PHARMACY
KHANAPUR, HAWELI, PUNE, MAHARASHTRA

DR. SUNITA DAHIYA
ORGANIZING CHAIRMAN
UNIVERSITY OF PUERTO RICO
SAN JUAN, PR, USA

INTERNATIONAL DAY OF HAPPINESS

S.D.D.V.C.P.&R.C.

2nd PharM March 22nd & 23rd, 2024
Panvel, Navi Mumbai, India
Meet of Academia Industry Regulatory

Operant Pharmacy Federation

2nd PharMAIR International Conference on "Pharm360: Emerging Trends and Future Perspectives in Pharmaceuticals"
22nd - 23rd March 2024

CERTIFICATE

OF PRESENTATION

This is to certify that Mr. Dinesh Dayaramji Chakole has presented E-Poster/Oral Presentation paper entitled Precision Drug Delivery through Methotrexate and Tofacitinib Citrate In Mesoporous Silica Co-Authored by Vishal V. Pande, Amol S. Rakte, Kothawade Sachin N. during **2nd PharMAIR International Conference** on **Pharm360: Emerging Trends and Future Perspectives in Pharmaceuticals** organised by **Shri. D. D. Vispute College of Pharmacy & Research Center, Panvel** and hosted by **Operant Pharmacy Federation** on 22nd & 23rd March 2024.

Dr. Vikram Choudhary
LOC Chairman

Dr. Ashish Jain
LOC Convener

Dr. Bhushan Rane
LOC Organising Secretary

Conference ID:MAIRPNVL

Certificate ID: PTC-103